Acta Chemica Scandinavica A 35 (1981) 497–508

Vibrational Spectra and Electronic Structure of Phosphinetriyltriacetonitrile, $P(CH_2CN)_3$

G. BORCH,[a] O. DAHL,[b] P. KLÆBOE[c] and P. H. NIELSEN[b]

[a] Chemistry Department A, The Technical University of Denmark, DK-2800 Lyngby, Denmark, [b] Chemical Laboratory II, The H. C. Ørsted Institute, DK-2100 Copenhagen, Denmark, and [c] Department of Chemistry, University of Oslo, Oslo 3, Norway

Infrared and Raman spectra have been recorded for $P(CH_2CN)_3$ and $P(CD_2CN)_3$ in the region below 4000 cm^{-1} in the solid state, (partly) as a melt, and in solution. The fundamental frequencies have been assigned in terms of C_3 symmetry on the basis of Raman depolarisation data and the results of a full normal coordinate analysis using a 22 parameter generalised valence force field. The torsional frequency was not identified. The assignments have been supported by comparison with infrared data for $X=P(CH_2CN)_3$, X = O,S,Se.

The effects of the CN groups on the electron density in $P(CH_2CN)_3$ (when compared to $P(CH_3)_3$) are discussed. The introduction of CN groups results in increased force constants for all PC_3 vibrations, and CNDO/2 calculations indicate a reduced electron density around phosphorus. It is concluded that the changes are best described in classical terms as a combination of inductive and field effects of the CN groups.

In a recent series of investigations [1-3] attention has been directed towards tertiary phosphines substituted with the cyanomethyl group. The results to date confirm the expectation that this group reduces the nucleophilic reactivity of phosphines, as shown by reduced rate constants for reactions with ethyl iodide in acetone. The low reactivity could be correlated with an increase in the lone pair ionisation potential of phosphorus.

An outstanding example of these compounds is phosphinetriyltriacetonitrile, $P(CH_2CN)_3$, which is a low-molecular weight aliphatic phosphine, but nevertheless crystalline, air-stable and with a very low nucleophilic reactivity. An X-ray analysis [3] of the crystal and molecular structure of $P(CH_2CN)_3$ shows that each molecule has C_3 symmetry. Orientation of the CN groups at approximately right angles to each other suggests minimisation of the repulsion of the CN dipoles as an important factor in determining the geometry. The X-ray analysis gave the unexpected result that the P–C bond length and C–P–C bond angle were almost identical with those found for $P(CH_3)_3$ in the gas phase. A slight elongation of the P–C bond and a small decrease of the C–P–C angle in $P(CH_2CN)_3$ relative to $P(CH_3)_3$ suggest a rehybridisation with increased *p*-character of the P–C bonds and increased *s*-character of the phosphorus lone pair. However, this effect seems to be much too small to explain the reduced reactivity and the increase in lone pair ionisation potential from $P(CH_3)_3$ (8.6 eV) to $P(CH_2CN)_3$ (10.6 eV) and indicates an additional inductive electron withdrawal to operate in the latter compound.

The main purpose of the present investigation is to gain information on the electronic distribution in $P(CH_2CN)_3$ relative to $P(CH_3)_3$ from a normal coordinate analysis (NCA). Further insight has been sought from CNDO/2 calculations on $P(CH_2CN)_3$ and $P(CH_3)_3$.

The vibrational spectra of $P(CH_2CN)_3$ and $P(CD_2CN)_3$ have been recorded in the solid state, as a melt and in solution and the spectra assigned. The force constants within the generalised valence force field (GVFF) approximation have been calculated from a full NCA. The changes in force constants from $P(CH_3)_3$ to $P(CH_2CN)_3$ in the solid state and in solution are discussed. The infrared spectra of the series $X=P(CH_2CN)_3$ (X = O, S, Se) were also recorded and proved very useful for confirming part of the assignment of the spectrum of $P(CH_2CN)_3$.

0302-4377/81/070497-12 $02.50 ·

STRUCTURE

$P(CH_2CN)_3$. The X-ray data[3] for the heavy atoms were used directly throughout all calculations. The position of the hydrogen atoms were estimated by assuming standard H–C distances, retention of the C_3 molecular symmetry and using the positions suggested by the X-ray results as a guide. The final coordinates may be obtained from the authors on request.

The vibrational spectra (Table 2 and 3) are almost unchanged on melting and it is reasonable to assume that most of the close contacts present in the solid are preserved in the melt. When the spectra are recorded in solution, shifts are observed which are compatible (see below) with a disappearance of the intermolecular forces operating in the solid state. No great changes, however, are found between NMR spectra of $P(CH_2CN)_3$ recorded as a melt and in solution. ^1H and ^{13}C NMR spectra in acetone show one doublet for CH_2 and one for CN ($^2J_{PH}$ 5.0 and $^2J_{PC}$ 5.7 Hz, respectively) and ^{13}C NMR of melted $P(CH_2CN)_3$ displays also one CN doublet ($^2J_{PC}$ 5.5 Hz at 130 °C). The ^1H NMR data show that the CH_2 hydrogens are magnetically equivalent in solution, probably due to fast interconversions between enantiomeric conformations (Fig. 1). The ^{13}C NMR data show that the dihedral angle between the lone pair and the C–C bond is almost the same in the melt and in solution, since $^2J_{PC}$ is known to be very dependent on the dihedral angle.[4,5] Therefore we conclude from the NMR data that the 'frozen' racemic mixture of conformers in the solid state[3] changes to a dynamic mixture of the same (or very similar) conformers in the melt and in solution. Consequently, the shifts observed in the vibrational spectra are probably not related to conformational changes in $P(CH_2CN)_3$.

$O=P(CH_2CN)_3$. A partial X-ray analysis has established that $O=P(CH_2CN)_3$ is isostructural to $P(CH_2CN)_3$. Both hexagonal axes increase by a very small amount (less than 0.2 Å). For crystallographic reasons it can be concluded that the structure of $O=P(CH_2CN)_3$ can be derived from that of $P(CH_2CN)_3$ simply by replacing phosphorus and its lone pair with a P=O group while the C_3 axis is preserved. The consequences of this are much smaller than expected and the results indicate that the space-filling properties of P: and P=O are comparable. Intuitively one would expect a lengthening of the unit cell along the c axis to allow for the space occupied by the oxygen atoms.

The oxygen atom of $O=P(CH_2CN)_3$ is perhaps "smaller" than usual because of increased $p_\pi - d_\pi$ back-donation in the oxide (which is equivalent to bending the p-orbitals towards phosphorus[6]). Besides, the electrostatic attraction between the $P(CH_2CN)_3$ hydrogen atoms and the P lone pair of the contiguous molecule becomes shorter and stronger when the lone pair is replaced by a negatively charged oxygen. By analogy to the structural changes observed in the series $(CH_3)_3P$,[7] $(CH_3)_3P=X$(X=O, S, Se),[8] we may also expect the introduction of oxygen in $P(CH_2CN)_3$ to result in an opening of the C–P–C angle and a slight shortening of the P–C bond. This effect contributes to providing more space for the P=O bond in $O=P(CH_2CN)_3$.

$S=P(CH_2CN)_3$ and $Se=P(CH_2CN)_3$. Partial X-ray analyses show that both crystal structures are different from those of $P(CH_2CN)_3$ and $O=P(CH_2CN)_3$. The sulfide and selenide are not isostructural either, although they belong to the same space group ($P2_1/n$), which however gives no indication on the molecular symmetry. Approximate unit cell dimensions are: $a=6.4$, $b=10.0$, $c=13.8$ Å, $\beta=93.3°$ for $S=P(CH_2CN)_3$, and $a=8.00$, $b=13.12$, $c=8.65$ Å, $\beta=91.25°$ for $Se=P(CH_2CN)_3$.

EXPERIMENTAL

Instrumental. The techniques and equipment used for recording the infrared and Raman spectra have been described in some detail previously.[9] Certain infrared spectra were also recorded on a Perkin-Elmer model 580 spectrometer in the region 4000 cm^{-1} to 180 cm^{-1}. The far infrared spectra were recorded with a fast scan Fourier transform interferometer (model 114 c) from Bruker. Beamsplitters of Mylar having thicknesses 3.5, 6 and 12 μm were employed, covering the region 600–40 cm^{-1}. A TGS far infrared detector combined with a globar and a mercury source were employed above and below 150 cm^{-1}, respectively. None of the useful solvents (acetonitrile, dimethylsulfoxide or water) can be employed in the far infrared region and this range was therefore investigated with polyethylene pellets or Nujol mulls only.

The Raman spectra were obtained using both green (5145 Å) and blue (4880 Å) laser excitation lines. The spectra of $P(CH_2CN)_3$ as a melt were of a rather poor quality because of the presence of small amounts of impurities, and polarisation measurements were not carried out. Attempts were made to record the Raman spectrum of $P(CH_2CN)_3$ in

aqueous solution, but with no success, probably due to the low solubility. Since the deuterium of $P(CD_2CN)_3$ was only very slowly interchanged with hydrogen at room temperature even in DMSO, the recording of these spectra did not present difficulties. When dissolved in acetone or acetonitrile, $P(CH_2CN)_3$ and $P(CD_2CN)_3$ are very easily oxidised to the corresponding phosphine oxides which are almost insoluble. Degassing of solvents and preparation under nitrogen gave solutions which were satisfactory for recording the infrared spectra. In order to get good quality Raman spectra the solutions were left for a few days to allow minute amounts of phosphine oxides to settle.

Chemicals. Phosphinetriyltriacetonitrile, $P(CH_2CN)_3$, was prepared as previously described.[3] The compound was more than 99 % pure according to ^1H and ^{31}P NMR.

Thiophosphoryltriacetonitrile, $S=P(CH_2CN)_3$. A mixture of $P(CH_2CN)_3$ (302 mg, 2 mmol), S_8 (64 mg, 2 mmol) and DMF (1 ml) was heated with stirring under N_2 to 125 °C for 1 h. The solvent was evaporated *in vacuo* and the residue recrystallised from H_2O. Yield 314 mg (86%), m.p. 132–133 °C. (Found: C 39.15, H 3.19, N 22.83, S 17.46. Calc. for $C_6H_6N_3PS$: C 39.34, H 3.30, N 22.94, S 17.51%). NMR ($(CD_3)_2SO$): δ_P 35.1, δ_H 4.00 (*d*, $^2J_{PH}$ 14.2 Hz).

Selenophosphoryltriacetonitrile, $Se=P(CH_2CN)_3$. A mixture of $P(CH_2CN)_3$ (151 mg, 1 mmol), red Se (79 mg, 1 mmol) and DMF (0.5 ml) was heated with stirring under N_2 to 100 °C for 5 min. The solvent was removed *in vacuo* and the residue recrystallised from H_2O. Yield 163 mg (71%), m.p. 152.5 – 154.5 °C (dec.). (Found: C 31.16, H 2.55, N 18.14. Calc. for $C_6H_6N_3PSe$: C 31.32, H 2.63, N 18.26%). NMR ($(CD_3)_2SO$): δ_P 20.8 (*s*+*d*, $^1J_{PSe}$ 821 Hz), δ_H 4.17 (*d*, $^2J_{PH}$ 14.3 Hz).

Hexadeuterophosphinetriyltriacetonitrile, $P(CD_2CN)_3$, was obtained from $P(CH_2CN)_3$ by exchange with D_2O in the presence of Et_3N. A solution of $P(CH_2CN)_3$ (302 mg, 2 mmol) and Et_3N (0.1 ml) in D_2O (3 ml) was heated to reflux under N_2 for 1 h. After cooling, the crystals were isolated and the above treatment repeated. Two recrystallisations from D_2O gave the pure compound (242 mg, 77 %), m.p. 111–112 °C. (Found: C 45.65, D 7.62, N 26.68. Calc. for $C_6D_6N_3P$: C 45.85, D 7.70, N 26.74 %).

Hexadeuterophosphoryltriacetonitrile, $O=P(CD_2CN)_3$, was prepared from $P(CD_2CN)_3$ and H_2O_2 in D_2O in the same way as $O=P(CH_2CN)_3$.[1]

Hexadeuterothiophosphoryltriacetonitrile, $S=P(CD_2CN)_3$, was obtained by recrystallisation of $S=P(CH_2CN)_3$ three times from D_2O.

NORMAL COORDINATE ANALYSIS

Using the geometry determined by X-ray methods,[3] NCA for $P(CH_2CN)_3$ and $P(CD_2CN)_3$ was carried out. The phosphine has 16 atoms and therefore 42 normal modes of vibration. For C_3 symmetry these give rise to 14 *A* fundamentals which are infrared and Raman active (polarised) and to 14 (doubly degenerated) *E* fundamentals which are also infrared and Raman active (depolarised). The frequencies were calculated using symmetry coordinates which are simple combinations of the internal coordinates shown in Fig. 1. Redundant coordinates were eliminated automatically by the program. Wilson's *GF* matrix method was used in the form of the program designed by Snyder and Schachtschneider.[10] The frequencies were weighted by $(1/\lambda)$ in the least-squares routine. A GVFF which has proved successful for trimethylphosphine [11] and derivatives [12–14] was used in the calculations. The initial force field was supplemented with values from propionitrile [15] and alkanes.[16]

Several interaction constants were included in some of the initial calculations but were omitted in the final calculation for one of three reasons: (1) they did not appreciably improve the overall fit, (2) they were not well determined or (3) they were very small and could be removed without significant influence

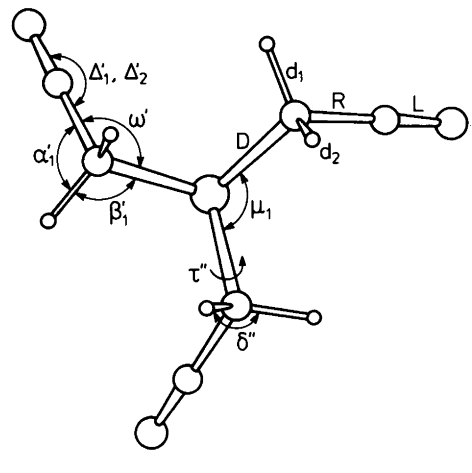

Fig. 1. Internal coordinates for phosphinetriyltriacetonitrile, $P(CH_2CN)_3$. The threefold axis of symmetry is perpendicular to the plane of the paper. The internal coordinates for the CH_2CN groups generated by the C_3 operation are designated ′ or ″ for convenience. The figure is given for the enantiomeric △-form.

Table 1. Final valence force constants for phosphinetriyltriacetonitrile.

Force type	Constants symbol	Coordinates involved	Value[a]	
			Solid state[b]	Solution[c]
Stretch	K_d	C–H	4.725	4.725
	K_D	C–P	3.219	3.387
	K_R	C–C	5.654	5.582
	K_L	C≡N	17.13	17.19
Stretch-stretch	F_d	C–H, C–H	0.010	0.011
	F_D	C–P, C–P	−0.135	−0.213
	F_{RD}	C–C, C–P	1.032	0.573
Bend	H_α	∠HCC	0.732	0.780
	H_β	∠HCP	0.482	0.473
	H_δ	∠HCH	0.482	0.490
	H_ω	∠CCP	0.881	1.01
	H_μ	∠CPC	1.343	1.503
	H_Δ	∠CCN	0.317	0.318
Stretch-bend	$F_{R\alpha}$	C–C, ∠HCC	0.288	0.378
	$F_{D\beta}$	C–P, ∠HCP	0.065	0.068
	$F_{D\omega}$	C–P, ∠CCP	0.608	0.798
Bend-bend	F_α	∠HCC, ∠HCC	−0.031	0.006
	F_β	∠HCP, ∠HCP	−0.029	−0.056
	$F'_{\alpha\beta}$	∠HCC, ∠HCP	0.038	0.032
	$f_{\beta\omega}$	∠HCP, ∠CCP	−0.061	−0.032
	F_μ	∠CPC, ∠CPC	0[d]	0.138
Torsion	H_τ	$NCCH_2-P$	0.03[d]	0.03[d]

[a] In units of mdyn/Å (stretch constants), mdyn/rad (stretch-bend interaction constants) and mdyn Å/(rad)^2 (bending and torsion constants). [b] Solid state geometry and fundamentals. [c] Solid state geometry and fundamentals from solution measurements. [d] Assumed and not varied.

on the agreement between observed and calculated frequencies. The final force constants are listed in Table 1. It should be noted that it was imperative to introduce the interaction force constant F_μ (CPC/CPC interaction) in order to reproduce the spectra observed in solution.

The final force constants for the $-CH_2CN$ group listed in Table 1 compare favourably with those reported for nitriles,[15] alkanes,[16] and methylphosphine.[17] The force constant for torsion of the P $-CH_2CN$ bond has deliberately been chosen small because the corresponding fundamental has not been observed, but probably has a higher value (*cf.* trimethylphosphine[12]). The force field pertaining the PC_3 group has been reported[11,12] for $P(CH_3)_3$ as K_D=2.91 mdyn/Å (C–P stretch), F_D= −0.034 mdyn/Å (C–P/C–P interaction), H_μ=0.833 mdyn·Å/(rad)^2 (C–P–C deformation) and F_μ very small (C–P–C/C–P–C interaction).

In $(CH_3)_3P$ adducts[13,14] as *e.g.* $(CH_3)_3P \cdot BH_3$ the force constant K_D for P–C stretching rises sharply to 3.65 mdyn/Å. This is attributed to an opening of the C–P–C angle (by 6°) followed by a rehybridisation of phosphorus approaching sp^3, an increase of C–P bond strength, and a decrease of the C–P bond length (by 0.02 Å). From Table 1 it is seen that the force constants of the PC_3 group (including K_D) increase in $P(CH_2CN)_3$ relative to $P(CH_3)_3$. However, in $P(CH_2CN)_3$ the C–P–C angle decreases by 1° and the P–C bond length increases by *ca.* 0.02 Å relative to $(CH_3)_3P$, *i.e.* in just the opposite direction of that found for the BH_3 adduct discussed above.

This result made us reconsider the arguments

indicating rehybridisation. The increase in P–C bond length by 0.02 Å has been taken to indicate an increased *p*-character of the phosphorus bonding orbital.[3] However, it is known that substitution of ethane with a cyano group to form propionitrile results in an increase of the C–C bond length from 1.534 [18] to 1.548 Å [19] and a similar influence of the cyano group can be expected. The remaining geometric changes could be explained by crystal packing effects occurring in $P(CH_2CN)_3$. We therefore believe rehybridisation in $P(CH_2CN)_3$ to play an insignificant role and attribute the dominant influence of the cyano group to be of electronic character. This will be discussed further below in connection with the CNDO/2 results.

When $P(CH_2CN)_3$ is dissolved in the polar solvents acetonitrile or dimethylsulfoxide, various spectral changes occurred (Tables 2 and 3) relative to the crystal spectra. These variations are also apparent in the force field (Table 1) and reflect the removal of the strong intermolecular forces in the crystal [3] (i) from the hydrogen atoms of the C–H bonds and the nitrogen of the cyano groups to the cyano groups of the neighbouring molecules, and (ii) from the lone pair of phosphorus to the hydrogen atoms of the contiguous molecule. However, the force field will also be highly influenced by simultaneous changes in symmetry, in geometry and in the appearance of external (lattice) modes in the low frequency region. We shall therefore only comment upon the changes in the force constants of the PC_3 group on dissolution. Not only are the values of K_d, F_d and H_μ (numerically) higher in solution than in the solid state, but in order to obtain a good fit between the observed and calculated frequencies in solution it was necessary to include the interaction force constant F_μ.

All these changes indicate an increased electron density around phosphorus, consistent with the changes expected from the effect (ii) above. The removal of the intermolecular forces is probably responsible for the upward shift of the CH/CD deformations, but the corresponding changes in force constants are irregular.

RESULTS AND DISCUSSION

The infrared spectrum of $P(CH_2CN)_3$ is shown in Fig. 2. The observed and calculated vibrational frequencies are listed in Table 2 together with a tentative assignment of the spectra and description of the fundamentals. The infrared spectrum displays a rich region of overtones and combination modes. However, most of these have been omitted from the tabulated frequencies except when they can be identified with reasonable confidence or are of exceptional strength. The corresponding data for $P(CD_2CN)_3$ are given in Table 3.

Assignment of the spectra of $P(CH_2CN)_3$ and $P(CD_2CN)_3$. As predicted by the NCA, accidental degeneracies reduce the number of observed CH_2 stretching frequencies to two. In the spectra of $P(CH_2CN)_3$ the asymmetric mode falls near 2965 cm^{-1} while the symmetric mode is observed near 2920 cm^{-1}. The corresponding modes in the spectra of $P(CD_2CN)_3$ have been identified with the strongest bands in the appropriate frequency range as shown in Table 3. In the same region the CN stretching vibration (coupled with some C–C stretching according to the NCA) is easily discerned as a strong (to very strong) band virtually unaffected by deuteration. When the Raman spectrum of $P(CH_2CN)_3$ is recorded in DMSO, the very strong polarised band at 2246 cm^{-1} can be assigned to the CN stretching vibration of species *a*. A shoulder of medium strength is observed at 2239 cm^{-1}, which is probably depolarised and accordingly assigned to

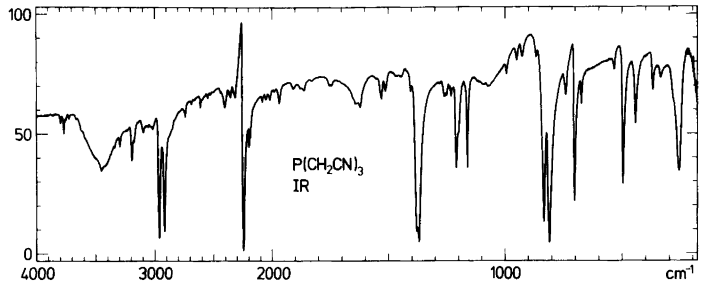

Fig. 2. Infrared spectrum of $P(CH_2CN)_3$ in the solid state in the region 4000 – 180 cm^{-1}.

Table 2. Observed[a] and calculated infrared and Raman frequencies (cm^{-1}) of $P(CH_2CN)_3$, tentative assignments of the spectra, and description of the fundamentals.

Infrared[b]			Raman[b]				Calculated[d]		Assignment and description[e]
Disc[c]	Solution CH_3CN/ CD_3CN	Solution CH_3COCH_3/ CD_3COCD_3	Solid	Melt	Solution		Solid	Solution	(PED, %)[f]
					CH_3CN	DMSO			
2965s	2958s	2956s	2967vs	2966s	2966w,sh,D?	2967w	2974	2974	ν_1a, $\nu_{as}CH_2$(100)
						2949m,D?	2974	2974	ν_{15}e, $\nu_{as}CH_2$(100)
2920s	2919s	2916s	2922vs	2922vs	2920m,sh,P?		2913	2913	ν_2a, ν_sCH_2(99)
							2913	2913	ν_{16}e, ν_sCH_2(99)
2244vs		2247s	2248vs	2247vs		2246vs,P	2242	2243	ν_3a, νCN(87), νCC(13)
		2240s,sh				2239m,sh,D?	2242	2243	ν_{17}e, νCN(87), νCC(13)
2195w			2198mw			2193w,P			
1619w	1625w		1621vw						$\nu_9+\nu_{21}$(E)
1380s	1399s	1402s	1381vs	1383m,br			1378	1398	ν_{18}e, δCH_2(99)
1370s	1392s,sh	1394s,sh	1373m,sh	1372m,sh		ca. 1390w,sh	1378	1398	ν_4a, δCH_2(99)
1249w	1250m		1243vw						
1209m	1232m,sh		1210vs	1212m	1231vs,D?	1231s,P	1212	1233	ν_{19}e, ωCH_2(60), tCH_2(40)
1199m,sh	1223s		1200s,sh	1202m,sh	1220vs,P?	1223s,P	1208	1225	ν_5a, ωCH_2(54), tCH_2(47)
	1212m,sh				1215m,sh,D?	1210m,sh			$\nu_8+\nu_{25}$(E)
1170vw	1200m,sh		1186w		1195m,sh,D?	1188w,sh			$\nu_9+\nu_{24}$(E)
1161m	1180m		1159s	1162w	1180w,D	1177w,sh,D?	1160	1178	ν_{20}e, tCH_2(63), ωCH_2(36)
1156w,sh	1166m,sh		1154m,sh		1167w,sh,P?	1165w,sh,P?	1154	1168	ν_6a, tCH_2(56), ωCH_2(44)
993w			997vw						$2\cdot\nu_{24}$(A+E)
951w	954vw,sh		949s	948vw	954w,sh,D?	949w,sh	947	950	ν_{21}e, νCC(72), νCN(11)
929w	939w		931m		940w,sh		940	948	ν_7a, νCC(78) νCN(11)
868w	866m,sh		870vw						$\nu_{24}+\nu_{25}$(A+E)
833s	853s	855s	837s	836w	861vw,D	859w,D?	835	853	ν_{22}e, ρCH_2(68), ν_{as}PC(14), νCC(9)
810vs	824s	825s	812s	812w	832w,D	833w,P?	816	838	ν_8a, ρCH_3(88)
	781w	784w	783vw		780w,P?				$\nu_{24}+\nu_{26}$(A+E)
741mw	746w	746w	745w			746m,sh,D?			$2\cdot\nu_{11}/2\cdot\nu_{25}$(A+E)
702s	707m	706m	705vs	705m	713vs,D		708	714	ν_{23}e, ν_{as}PC(83), ρCH_2(16)
694m,sh	694w	696w,sh			695vs,D				$\nu_{12}+\nu_{25}$(E)
	686w	687w			673s,sh,P?				$\nu_{11}+\nu_{12}$(A)
674mw	668vw,sh		676vs	676m	664vs,P		678	666	ν_9a, ν_sPC(87), δCCP(21)
534w	530w		528vw						$2\cdot\nu_{26}$(A)
495ms	512m		500s	496m	522w,D?	517w,D?	503	517	ν_{24}e, δCCN(46), δCCP(39)
	506m,sh				512vw	512w,D?			$\nu_{13}+\nu_{25}$(E)
	485w				490w,D	488w,D?			$\nu_{12}+\nu_{27}$(E)

443m	454m	447vs	444m	457vs,P	459s,P	445	460	ν_{10}a, δCCN(54), δCCP(17), ν_sPC(14)
369mw		374vs	373m		370w,sh	364	365	ν_{11}a, δCCN(92)
						364	365	ν_{25}e, δCCN(92)
339w		338w	342w					$2\cdot\nu_{27}$(A+E)
283m		286m	287mw	311m,P		283	310	ν_{12}a, δCPC(71), ν_sPC(10)
260s		263m	267mw	263w,D	263w,D			ν_{26}e, δCPC(65), δCCN(21)
				239w,D	242w,D?			$\nu_{24}-\nu_{26}$(A+E)
170m		176vw	178w		177vw	166	168	ν_{27}e, δCCP(40), δCCN(33), δCPC(21)
153w,sh		145w,br	145w		150vw	138	142	ν_{13}a, δCCP(52), δCCN(34)
109s								
84s								
68s								lattice modes
59s								
42s								
						39	39	ν_{14}a, ν_{28}e, τCH$_2$CN(92)

[a] Several weak and very weak bands which are not assigned to fundamentals have been omitted from the table. [b] The following abbreviations have been used: s, strong; m, medium; w, weak; br, broad; sh, shoulder; P, polarised; D, depolarised. [c] 'Best' values from KBr, KI, CsI and polyethylene pellets. [d] Iteration based upon both isotopic species. [e] Abbreviations: ν=stretching, δ=deformation, ω=wagging, t=twisting, τ=torsion, and, as subscripts, s=symmetric, as=antisymmetric. The description is based upon calculations for the solid state. [f] The potential energy distribution (PED) is defined as $x_{ik}=100F_{ii}L_{ik}^2/\lambda_k$. The stated PED's are only approximative and small contributions have been neglected.

Table 3. Observed[a] and calculated infrared and Raman frequencies (cm^{-1}) of P(CD$_2$CN)$_3$, tentative assignments of the spectra, and description of the fundamentals.

Infrared[b]			Raman[b]			Calculated[d]		Assignment and description[e] (PED, %)[f]
Disc[c]	Solution CH$_3$CN/ CD$_3$CN	Solution CH$_3$COCH$_3$/ CD$_3$COCD$_3$	Solid	Solution CH$_3$CN	Solution DMSO	Solid	Solution	
2248vs		2248vs	2248vvs		2248vvs,P	2249	2248	ν_1a, νCN(80), νCC(14)
2243s,sh		2244s,sh				2250	2248	ν_{15}e, νCN(79), νCC(13)
2228s	2222s	2222s	2227vs	2226s,D	2215m,D	2214	2214	ν_2a, ν_{as}CD$_2$(97)
						2215	2215	ν_{16}e, ν_{as}CD$_2$(96)
2178m	2188w	2187w	2176vs	2191m,P	2187w,sh			$2\cdot\nu_{18}$(A)
2158w	2164vw	2168vw	2161vw	2167w,sh				$2\cdot\nu_4$(A)
2114m	2122m	2120m	2113vs	2121vs,P	2115vs,P	2123	2123	ν_3a, ν_sCD$_2$(93)
						2124	2124	ν_{17}e, ν_sCD$_2$(93)
2059w			2060vw	2077w,sh,D				$\nu_4+\nu_{19}$(E)
1690w				1710vw,P?				$2\cdot\nu_{21}$(A+E)

Table 3. Continued.

1073s	1092m 1084s		1076s	1092m,sh,D 1084m,P	1085m,P?	1073 1071	1091 1081	ν_{18}e, δCD_2(21), νCC(51), ωCD_2(44) ν_4a, δCD_2(25), νCC(49), ωCD_2(42)
989s	994m,sh		989vs		995m,sh,D?	992	1002	ν_{19}e, δCD_2(50), ωCD_2(32), ν_{as}PC(25)
980s,sh	989s	989s	981s,sh	992vs,P	991m,P?	971	978	ν_5a, δCD_2(50), ωCD_2(34), ν_sPC(14)
881w,sh	900w,sh		886w,sh	890w,sh,D?		881	892	ν_{20}e, tCD_2(90)
878mw	884w		879w	887vw,D?	884vw,sh	876	887	ν_6a, tCD_2(94)
843w,sh	850vw,sh		848m,sh	853m,sh,D	854w,sh,D	845	846	ν_{21}e, ωCD_2(26), νCC(30), ν_{as}PC(11)
836m	841m	840m	842s	844vs,P	846m,P	832	844	ν_7a, ωCD_2(41), νCC(28), ν_sPC(8)
826w,sh	832vw,sh		837m,sh					$\nu_{11}+\nu_{24}$(E)
774mw	781w							$\nu_{10}+\nu_{11}$(A)
747m,sh			748w,sh					$\nu_9+\nu_{27}$(E)
732s	734s	735s	735m	740m,D	742vw,D?			$\nu_{24}+\nu_{26}$(A+E)
702vs	720s	720s	705s	726m,D		700	720	ν_{22}e, ρCD_2(38), ν_{as}PC(24)
669mw	698m	699m	663w	692w,P?		664	692	ν_8a, ρCD_2(66), ν_sPC(18)
	687m	688m		682w,D?				$\nu_{10}+\nu_{26}$(E)
	676w,sh	676m,sh						$2\cdot\nu_{11}$(A)
639w	640w,sh	641w	637w,sh	642w,sh,D				$\nu_{13}+\nu_{24}$(E)
587m	626mw	624mw	590s	631m,D?		602	614	ν_{23}e, ρCD_2(44), ν_{as}PC(42)
	612w,sh	614w,sh		615s,P	615m,sh			$\nu_{11}+\nu_{12}$(A)
611m	592vw	590vw	614s	593s,P	597m,P	612	599	ν_9a, ν_sPC(49), ρCD_2(20)
491ms	504m		494m	502w,D?	500w,D?	493	502	ν_{24}e, δCCP(38), δCCN(47)
	496m,sh							$\nu_{11}+\nu_{27}$(E)
475m,sh	477mw		475w,sh	480m,P	480m,P			$2\cdot\nu_{26}$(A+E)
441ms	449m		444vs	452vs,P	454vs,P	443	457	ν_{10}a, δCCN(53), δCCP(16), ν_sPC(15)
337m,sh								
332s			338s	341s,D		339 341	340 342	ν_{11}a, δCCN(89) ν_{25}e, δCCN(89)
320w,sh								$2\cdot\nu_{27}$(A+E)
260m,sh			258w	288m,P		261	285	ν_{12}a, δCPC(67), ν_sPC(10)
244s			240m	243m,D	248w,D	245	248	ν_{26}e, δCPC(56), δCCN(22), δCCP(10)
195vw			205vw	220mw,D	220vw,D?			$\nu_{10}-\nu_{26}$(E)
161m			162w			157	157	ν_{27}e, δCCP(37), δCPC(29), δCCN(28)
145w,sh			142w,sh			134	138	ν_{13}a, δCCP(52), δCCN(32)
130m								
105vs			125w					lattice modes
71s			90w					
62m								
						37	37	ν_{14}a, ν_{28}e, τCD_2CN

[a,b,c,d,e,f] See footnotes to Table 2.

the CN stretching vibration of species *e*. However, we want to point out that several overtones and combination modes of species *e* occur near this frequency (*e.g.* $\nu_6+\nu_{20}$, $2\cdot\nu_{20}$) and might explain the occurrence of this band.

In the region 800 – 1400 cm^{-1} in the spectrum of $P(CH_2CN)_3$ a total of ten fundamentals are observed. From Table 2 it is seen that they are grouped two by two in a characteristic way. First, polarisation measurements in the Raman spectra of CH_3CN and DMSO solutions suggest that each pair consists of one fundamental of species *a* and one of species *e*. Second, the fundamental of species *e* is in all cases situated at the highest frequency. Third, four of these pairs (near 1375, 1205, 1160 and 820 cm^{-1} in the solid state) are displaced towards higher frequencies in the solution spectra, while one of these pairs has almost unchanged frequency (929 – 954 cm^{-1}).

The observations strongly indicate that the four former bands are due to the internal vibrations of the CH_2 group expected in this region ($\delta,\omega,t,\rho CH_2$), while the latter band originates in C – C stretching. The upwards frequency shift of the former bands in the solution spectra is qualitatively explained by the disappearance of the strong intermolecular forces to the hydrogen atoms in the solid state. All these predictions are confirmed by the results of the NCA which also show that the wagging and twisting motions of CH_2 are strongly coupled in $P(CH_2CN)_3$. In the corresponding region (650 – 1100 cm^{-1}) of the spectra of $P(CD_2CN)_3$ five similar pairs of bands occur, but in this case the solution shifts are smaller and the C – C stretching motion is coupled to the inner vibrations of the CD_2 group (Table 3).

The asymmetric P – C stretching frequency is found (weakly coupled to CH_2 rock) in the solid state spectra of $P(CH_2CN)_3$ at 702 – 705 cm^{-1}, while the corresponding symmetric mode (coupled weakly to CCP deformation) is observed near 675 cm^{-1}. In the spectra of $P(CH_2CN)_3$ in solution, $\nu_{as}PC$ is displaced by 4 – 8 cm^{-1} towards higher frequencies, but ν_sPC by 6 – 12 cm^{-1} in the opposite direction resulting in an increased splitting of the two bands in solution by 10 – 20 cm^{-1}. Qualitatively this points to an increased P – C/P – C interaction in solution and this is confirmed by the NCA (Table 1).

The situation is much more complicated in the case of $P(CD_2CN)_3$ as is apparent from Table 3. Both the asymmetric and the symmetric P – C stretching motion appears to be coupled quite strongly to other vibrations and contribute to fundamentals in the range 250 – 1000 cm^{-1}. Furthermore, the bands with maximum P – C stretching character (near 600 cm^{-1}) show a complicated behaviour when going from the spectra of the solid state to those in solution. The fundamental $\nu_{23}e$ is displaced from 587 – 590 cm^{-1} to 624 – 631 cm^{-1}, but ν_9a is at the same time displaced in the opposite direction from 611 – 614 cm^{-1} to 590 – 597 cm^{-1} with the result that the two fundamentals change place. This assignment, of course, has not been verified experimentally but turned out to be a necessary prerequisite to obtain a reasonable fit in the NCA.

In the low frequency region, the CCP deformation, the CPC deformation and one of the CCN deformations couple rather strongly to each other and give rise to a total of 6 fundamentals, three of each species. The four highest of these (ν_{10}, ν_{12}, ν_{24}, and ν_{26}) have been identified by Raman polarisation measurements in solution, but $\nu_{13}a$ and $\nu_{27}e$ in the 100 – 200 cm^{-1} region have been assigned in accordance with the NCA. One of the CCN deformations is orthogonal to most of the other vibrations and the mode gives rise to the accidentally degenerate ν_{11} and ν_{25} near 370 cm^{-1} in $P(CH_2CN)_3$ and near 340 cm^{-1} in $P(CD_2CN)_3$.

The infrared spectra of $X=P(CH_2CN)_3$ *(*$X=O, S, Se$*).* In the region above 800 cm^{-1} the spectra run in KBr/CsI discs were dominated by bands which could be identified easily by comparison with the spectra of $P(CH_2CN)_3$ as due to $\delta,\omega,\nu,t,\rho CH_2$ and νCC. In addition the spectra of $O=P(CD_2CN)_3$ and $S=P(CD_2CN)_3$ were recorded and proved similar in the same respects to those of $P(CD_2CN)_3$. The P=O stretching vibration was unambiguously identified by its intensity and position in the spectrum of $O=P(CD_2CN)_3$ at 1212 cm^{-1} (KBr). The spectra of $S=P(CH_2CN)_3$ and $Se=P(CH_2CN)_3$ (KBr) differed in many details from those of $O=P(CH_2CN)_3$ as expected from the change in crystal structures. An IR spectrum run in CD_3CN solution of $S=P(CH_2CN)_3$ was much simpler than the spectrum recorded in the solid state, indicating the presence of strong intermolecular interactions and/or reduced molecular symmetry in the crystal. Therefore, we desist from a discussion of these bands without more complete information about the structures in the solid state.

The values recorded for the most important infrared bands in the solid state below 800 cm^{-1} are tabulated in Table 4. For convenience, the data

Table 4. The most important infrared bands (cm^{-1}) in the region below 800 cm^{-1} (CsI discs) for $X=P(CH_2CN)_3$ ($X=O$, S, Se) and $X=P(CD_2CN)_3$ ($X=O$, S). The description is based upon the corresponding bands for $P(CH_2CN)_3/P(CD_2CN)_3$.

$P(CH_2CN)_3$	$O=P(CH_2CN)_3$	$S=P(CH_2CN)_3$	$Se=P(CH_2CN)_3$	$P(CD_2CN)_3$	$O=P(CD_2CN)_3$	$S=P(CD_2CN)_3$	Approximate description
702s	724m	719s	715m				$\nu_{as}P-C$ (E)
674mw	678mw	699m	690mw				ν_sP-C (A)
		626s	526s			587s	$\nu P=S/\nu P=Se$ (A)
495ms	540s	523m	495m	491ms	529s	506m	$\delta CCN+\delta CCP$ (E)
443m	431mw	430mw	397m	441ms	433m	429mw	$\delta CCN+\delta CCP$ (A)
369mw	361mw	366mw	365mw	332s	342m	335mw	δCCN (A+E)
	340s	286s			322s	272s	$\delta CPO/\delta CPS$ (E)
283m	291m		278m	260m	267m		δCPC (A)
			240m				$\delta CPSe$ (E)
260s	240s	228m	219s	244s	228m		δCPC (E)

obtained for $P(CH_2CN)_3/P(CD_2CN)_3$ are included together with a short description of the bands based upon the NCA of the latter compounds. Most of the variations follow closely those reported for the corresponding derivatives of $(CH_3)_3P$ [12] and will not be discussed here. However, we wish to point out that many displacements may be explained by coupling to either the P=X (X=O, S, Se) stretching coordinate of species *A* or the C–P=X deformation coordinate of species *E*. For example, the displacement of the symmetric P–C stretching vibration towards higher frequencies in $S=P(CH_2CN)_3$ is explained by coupling to the P=S stretching coordinate introduced at 626 cm^{-1}.

The introduction of the C–P=X deformation coordinate in the 240–340 cm^{-1} region causes considerable displacement of both the δCPC band at 219–260 cm^{-1} and the $\delta CCN+\delta CCP$ band at 491–540 cm^{-1}, which are both of species *E*. On the other hand, the δCCN band at 369 cm^{-1} in $P(CH_2CN)_3$ and 332 cm^{-1} in $P(CD_2CN)_3$ are almost unaffected in $X=P(CH_2CN)_3/X=P(CD_2CN)_3$ as expected. Therefore, the results of Table 4 support the assignments given for $P(CH_2CN)_3$ in Table 2 and $P(CD_2CN)_3$ in Table 3.

We call attention to the fact that both the asymmetric and the symmetric P–C stretching frequencies are raised in the spectra of $O=P(CH_2CN)_3$ relative to $P(CH_2CN)_3$. In the case of $\nu_{as}P-C$, $\delta C-P=O$ is not expected to couple to any significant extent since it is found at much lower frequencies. In the case of ν_sP-C, any coupling with $\nu P=O$ would tend to decrease the frequency since $\nu P=O$ is found at higher frequencies. The increase in both P–C stretching frequencies therefore indicates a larger P–C stretching force constant, *i.e.* a stronger P–C bond as predicted from similar results for $O=P(CH_3)_3$.[8]

CNDO calculations. In the ^1A ground state of $P(CH_2CN)_3$ the 50 valence electrons fill up the molecular orbitals $9a+8e$. CNDO/2 calculations were carried out on $P(CH_3)_3$ and $P(CH_2CN)_3$ in order to investigate the influence of the cyano group on the electron distribution. For $P(CH_3)_3$ both CNDO [20] and *ab initio* [21] calculations have been published indicating that the absolute values obtained by the CNDO/2 method are not very reliable. However, the CNDO method is often capable of accounting qualitatively for the experimentally determined trends. For example, we calculate an increase of the HOMO ionisation potential (using Koopman's theorem) from $P(CH_3)_3$

(11.9 eV) to $P(CH_2CN)_3$ (13.0 eV) compared to 8.6 and 10.6 eV, respectively, from experiments (PES). Calculations were also performed for $P(CH_3)_3$ using the same P–C bond length and C–P–C bond angle as in $P(CH_2CN)_3$. The results indicate that the geometry change can account for *ca.* 0.15 eV of the increase in IP for $P(CH_2CN)_3$. Examination of the HOMO's of $P(CH_3)_3$ and $P(CH_2CN)_3$ show that they are mostly phosphorus lone pairs, and that the additional stabilisation in $P(CH_2CN)_3$ is effected mainly by *ca.* 10 % transfer of electron density from phosphorus to the three CN groups. Since the percentage *s*-character on the HOMO of $P(CH_2CN)_3$ decreases both on a relative and an absolute scale, the increased IP cannot be explained by an increase in *s*-character of the lone pair.[3]

The overall effects of CN substitution on the electron distribution may be summarised as follows. Each of the cyano groups are strong dipoles with the positive end at C (+0.11 e) and the negative end at N (−0.17 e). In total, therefore, each CN group accumulates electron density (0.06 e) at the expense of both the CH_2 groups and phosphorus. At first this appears to contradict the NCA results. These indicate that both the P–C stretching and the C–P–C bending force constants increase from $P(CH_3)_3$ to $P(CH_2CN)_3$, which is difficult to reconcile with a diminished electron density on both P and CH_2. However, a closer inspection of the density matrix

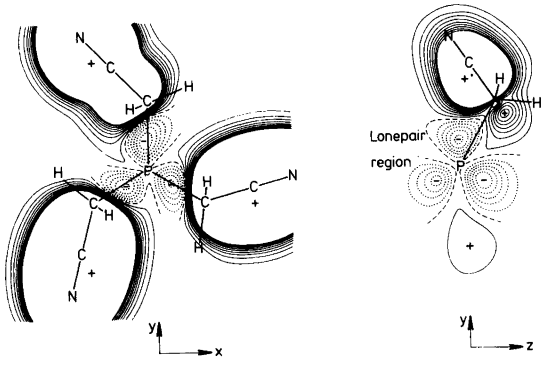

Fig. 3. Difference maps ($P(CH_2CN)_3 - P(CH_3)_3$) of the total molecular electron density in a plane through phosphorus viewed along the C_3 axis (left) and in a plane through the C_3 axis and one of the P–C bonds (right) as calculated by the CNDO/2 method. Solid, dashed and dotted lines represent positive, zero and negative difference densities, respectively, plotted linearly with a specing of 0.001 electron/Å^3. The geometry of $P(CH_2CN)_3$ is used for both molecules.

reveals that although there is a net decrease in density on both P and C of the P–C bond, the density actually increases in some of their orbitals. In order to get a more precise description of the changes we calculated difference contours (Fig. 3) displaying the difference in total electron densitity between $P(CH_2CN)_3$ and $P(CH_3)_3$ in two perpendicular planes through phosphorus. In both diagrams the regions of the CN groups are very conspicuous because they show the large difference between the electron density of CN and H. The density changes in the remaining regions reflect more adequately the introduction of the CN groups. From the density plot to the left, it is seen that the density decreases in the region nearest P in a direction along the projection of the P–C bonds. As the CH_2 groups are well away from the plane the plot shows little about the changes near these groups.

The density plot to the right of Fig. 3 is more informative. Firstly it shows the decreased density around phosphorus mentioned before; the decrease is considerable in most of the lone pair region in agreement with the low nucleophilic reactivity of $P(CH_2CN)_3$. In addition to the transfer to the CN groups electron density is transferred also to an area close to the CH_2 groups and opposite the CN bond. Secondly it is seen that the electron density in the P–C bond region is slightly decreased in one area and slightly increased in another. Similarly, in the space relevant to C–P–C bending (the right side of the plot) there are areas of increase as well as decrease in electron density. These changes in opposite directions give no indications whether the P–C stretching or the C–P–C bending force constants should increase (as is the case) or decrease. However, the calculations do show that it is possible for a force constant to increase at the same time as the total electron density at the atoms involved decreases. The overall effect of the CN groups may be summarized in classical terms as an inductive and a field effect. The transfer of electron density to the CN groups reflects the inductive effect, whereas the larger decrease in electron density around phosphorus than around CH_2 is most readily explained by a field effect.

Conclusion. The NCA on $P(CH_2CN)_3$ when compared to $P(CH_3)_3$ shows an increase in the force constants related to PC_3 vibrations. This increase is not a result of the small geometry (rehybridisation) changes but rather an effect of a redistribution of electron density induced by the CN groups. The

CNDO calculations indicate that electron density decreases in the lone pair region and increases in an area near CH_2 and at CN, but give little information on the electron density changes which must be responsible for the change in the force constants. The decrease in electron density in the lone pair region, which is considered responsible for the low nucleophilic reactivity and the high lone pair IP of $P(CH_2CN)_3$, is best explained in classical terms by a field effect of the CN groups.

Acknowledgements. We are grateful to Dr. Sine Larsen and to Flemming Hansen who kindly provided the crystal structure data for X $= P(CH_2CN)_3$ and to Anne Horn who recorded part of the spectra. This research was supported by the Danish Natural Science Research Council and the Norwegian Research Council for Science and the Humanities.

REFERENCES

1. Dahl, O. *Acta Chem. Scand. B 30* (1976) 799.
2. Dahl, O. and Henriksen, L. *Acta Chem. Scand. B 31* (1977) 427.
3. Dahl, O. and Larsen, S. *J. Chem. Res. (S)* (1979) 396, (M) 4645.
4. Dutasta, J. P. and Robert, J. B. *J. Chem. Soc. Chem. Commun.* (1975) 747.
5. Breen, J. J., Featherman, S. I., Quin, L. D. and Stocks, R. C. *J. Chem. Soc. Chem. Commun.* (1972) 657.
6. Wallmeier, H. and Kutzelnigg, W. *J. Am. Chem. Soc. 101* (1979) 2804.
7. Lide, D. R., Jr. and Mann, D. E. *J. Chem. Phys. 29* (1958) 914; Bartell, L. S. and Brockway, L. O. *J. Chem. Phys. 32* (1960) 512.
8. Cogne, A., Grand, A., Laugier, J., Robert, J. B. and Wiesenfeld, L. *J. Am. Chem. Soc. 102* (1980) 2238; Wilkins, C. J., Hagen, K., Hedberg, L., Shen, Q. and Hedberg, K. *J. Am. Chem. Soc. 97* (1975) 6352.
9. Anthoni, U., Nielsen, P. H., Borch, G., Gustavsen, J. and Klæboe, P. *Spectrochim. Acta A 33* (1977) 403.
10. Snyder, R. G. and Schachtschneider, J. H. *Spectrochim. Acta 19* (1963) 85.
11. Bouquet, G. and Bigorgne, M. *Spectrochim. Acta A 23* (1967) 1231.
12. Rojhantalab, H., Nibler, J. W. and Wilkins, C. J. *Spectrochim. Acta A 32* (1976) 519.
13. Odom, J. D., Hudgens, B. A. and Durig, J. R. *J. Phys. Chem. 77* (1973) 1972.
14. Odom, J. D., Chatterjee, K. K. and Durig, J. R. *J. Phys. Chem. 84* (1980) 1843.
15. Yamadera, R. and Krimm, S. *Spectrochim. Acta A 24* (1968) 1677.
16. Schachtschneider, J. H. and Snyder, R. G. *Spectrochim. Acta 19* (1963) 117.
17. Lannon, J. A. and Nixon, E. R. *Spectrochim. Acta A 23* (1967) 2713.
18. Allen, H. C., Jr. and Plyler, E. K. *J. Chem. Phys. 31* (1959) 1062.
19. Lerner, R. G. and Dailey, B. P. *J. Chem. Phys. 26* (1957) 678.
20. Kuznesof, P. M., Pessine, F. B. T., Bruns, R. E. and Schriver, D. F. *Inorg. Chim. Acta 14* (1975) 271.
21. Hillier, I. H. and Saunders, V. R. *Trans. Faraday Soc. 66* (1970) 2401.

Received December 17, 1980.